

Interpretation of SPM images of Langmuir–Blodgett films based on long-chain carboxylic acids

G.K. Zhavnerko^a, V.N. Staroverov^a, V.E. Agabekov^a, M.O. Gallyamov^b, I.V. Yaminsky^{b,*}

^a*Institute of Physical Organic Chemistry, Academy of Science of Belarus, ul. Surganova 13, Minsk 220072, Belarus*

^b*Department of Physics, Moscow State University, Vorobievsky Gory, Moscow 119899, Russia*

Received 8 November 1998; received in revised form 1 June 1999; accepted 23 September 1999

Abstract

A ‘horizontal precipitation’ method for preparation of uniform Langmuir–Blodgett (LB) films has been developed. The technique was successfully employed in scanning tunneling microscopy (STM) and atomic force microscopy (AFM) studies of dense cobalt behenate monolayers deposited on a graphite substrate. Experimental results were complemented by a theoretical simulation of STM images of long carbon chains using a zero-interaction model. The agreement between the observed and simulated distributions of the STM current indicates that the weak interactions between graphite and the adsorbed molecules may be negligible. © 2000 Published by Elsevier Science Ltd. All rights reserved.

Keywords: Langmuir–Blodgett films; Atomic force microscopy; Scanning tunneling microscopy; Computer simulation

1. Introduction

The scanning probe microscopy (SPM) is an attractive tool for probing the surface structure of molecular aggregates including such model prototypes of biological membranes as Langmuir–Blodgett (LB) films [1]. Under favorable conditions, STM gives an atomic resolution for non-conducting molecules adsorbed on a conducting substrate. The role of the substrate is most commonly played by highly oriented pyrolytic graphite (HOPG), which is also used as a standard specimen [2].

Every so often, the analytical signal detected in STM is transformed into images which cannot be trivially interpreted. In such cases it becomes necessary to invoke theory. Indeed, since the advent of STM technology, there has been a number of attempts to provide some theoretical basis for STM imaging of organic molecules on graphite surface [3–5]. Long ago, Tersoff and Hamann [3] showed that for a small bias in the constant current mode, the STM tip approximately follows the contour of constant local density of states at the Fermi level. However, in the presence of a thin organic (usually dielectric) layer between the tip and a conductive surface, calculation of the exact electron density distribution for the substrate-adsorbate system becomes a relatively complex problem. In one of the first attacks on this subject, Lippel et al. [4] showed a similarity between

the frontier molecular orbital electron density distribution and the STM image of copper-phthalocyanine molecules. A more rigorous approach to calculation of the tunneling current between the tip and the adsorbate/substrate system was developed later by Ou-Yang et al. [5–7] and applied to adenine molecules adsorbed on the graphite surface. A similar model has been employed for interpretation of STM images of LB films of behenic acid [8]. The purposes of the present work are: (1) to develop a technique for preparation of LB films with the horizontal arrangement of amphiphilic molecules; (2) to compare experimental STM images of the prepared samples with those predicted by theory.

2. Experimental

2.1. Instruments

The LB films were probed with an atomic-force microscope (AFM) and a scanning tunneling microscope (STM). AFM images were obtained using Nanoscope IIIa (Digital Instruments, USA) operated in the constant force mode (1.5–5 nN) in air at room temperature. Nanoprobe 100 and 200 μm cantilevers (with the spring constants 0.06, 0.12, 0.38, 0.58 N/m) with oxide-sharpened Si_3N_4 integral tips were used. AFM was equipped with a ‘D’ scanner, which was calibrated using mica and HOPG. We estimate the precision of the calibrating procedure at 3–5%. Data

* Corresponding author.

were collected at a scan speed of 5–15 Hz with an information density of 512×512 points. Molecular resolution was obtained by AFM at a scan speed of 60 Hz using cantilevers with a 0.38 N/m spring constant.

The tunneling microscope was an original instrument constructed by Moiseev and coworkers [9]. It was operated in air in the constant current mode with tungsten and PtIr tips. The STM was calibrated using the HOPG lattice to the precision of about 10%.

2.2. Materials and sample preparation

Behenic acid (Aldrich), cetylamine (CA) (Merck) and 5-[2-(4-octadecanamidobenzoyl)acetamido]-1,3-benzenedicarboxylic acid (DA) were used as film components. DA was synthesized via hydrogenation of 5-[2-(p-nitrobenzoyl)acetamido]isophthalic acid in ethanol over Raney nickel at 3×10^5 Pa, followed by condensation of the resulting amine with stearoylchloride in pyridine [10]. The final product was purified by crystallization from acetic acid and, additionally, by liquid chromatography (Silicagel L40/100) using acetone as the eluent.

The behenic acid monolayers were prepared by spreading 0.5–1 mM chloroform solutions either on bidistilled water or on an aqueous CoBr_2 (0.5 mM) solution. Mixtures of DA with CA were used in an acetone-chloroform (1:1 vol.) solution (0.5–0.6 mM). Surface pressure vs. area per molecule (π -A) isotherms were measured at a compression speed of $0.2 \text{ \AA}^2/(\text{molecule min})$. Films were deposited on a freshly cleaved HOPG or mica surface. Two types of mono- and multilayer films were prepared by:

1. standard LB ‘vertical’ procedure [11];
2. ‘horizontal precipitation’ procedure.

Method (2) includes the following steps:

- the substrate is placed horizontally in the trough and the trough is filled with water (or an aqueous CoBr_2 solution);
- a monolayer is formed by spreading a solution of the film-forming compound on the aqueous surface and compressed to a ‘solid’ state;
- the monolayer is transferred onto an HOPG surface, and the water is allowed to slip off slowly (0.5–0.6 ml per minute), leaving a homogeneous film. The change of the surface pressure during the deposition was less than 2–3 mN/m.

Method (1) results in a Y-type deposition while method (2) leads to a Z-type film. Surface pressure during the deposition was maintained at 20, 30, or 50 mN/m.

The horizontal arrangement of hydrocarbon chains of DA molecules surface was obtained by deposition of a bicomponent mixture of DA and cetylamine (1:2 molar ratio) onto HOPG surface using a procedure known as the ‘thermal vacuum annealing’. In this technique, only the DA mole-

cules remain in the LB film after thermal vacuum desorption of CA molecules.

3. Calculation procedure

An accurate quantitative model of STM should include the structure of the tip. However, to a good approximation, the tip can be represented by a semi-infinite linear chain of metal atoms such as tungsten or platinum [6]. Assuming this model, Ou-Yang, Marcus and Källebring showed [5] that in the low-bias voltage limit the tunnel current is proportional to: (i) the sum of the tip-adsorbate Hamiltonian matrix elements taken over the adsorbate molecular orbitals involved in tunneling and over the atomic orbitals of the tip; (ii) the effective local density of states of the adsorbate/substrate system at the Fermi energy level, $\rho_{\alpha,0}$

$$I_{\text{ads}} \propto \sum_{\alpha,m} \left| \langle \phi_{\alpha} | \hat{H} | d_m^t \rangle \right|^2 \rho_{\alpha,0} \quad (1)$$

where d_m^t denotes the m -th d -orbital of the tip atom closest to the sample and ϕ_{α} is the α -th molecular orbital (MO) of the adsorbate involved in tunneling.

As pointed out by the authors [5], Eq. (1) implies that the overall image brightness of the adsorbed molecule depends on $\rho_{\alpha,0}$ whereas the relative contributions from different atoms depend mainly on the term containing tip-adsorbate Hamiltonian matrix elements. If molecular orbitals are written as linear combinations of certain basis functions,

$$\phi_{\alpha} = \sum_{i=1}^N c_i^{\alpha} \chi_i \quad (2)$$

where c_i^{α} are the MO coefficients determined from some preliminary calculation, then the expression for the tunneling current (I_{ads}) for a given tip-substrate distance is easily obtained by substitution of Eq. (2) into Eq. (1)

$$I_{\text{ads}} \propto \sum_{\alpha,m} \sum_{i,j=1}^N c_i^{\alpha} c_j^{\alpha} \langle \chi_i | \hat{H} | d_m^t \rangle \langle d_m^t | \hat{H} | \chi_j \rangle \rho_{\alpha,0} \quad (3)$$

We calculated and plotted the values of I_{ads} as a function of the tip position over the adsorbate in the approximation of constant local density of states $\rho_{\alpha,0}$ MO energies and MO expansion coefficients were calculated by the extended Hückel theory (EHT) [12], which treats valence electrons only. The basis functions used here were Slater-type orbitals with fixed exponents. The values of ionization potentials, Slater exponents and empirical parameters required in EHT were taken from the literature [12–14].

4. Results and discussion

4.1. AFM experiments

We prepared two structurally different types of high quality LB films:

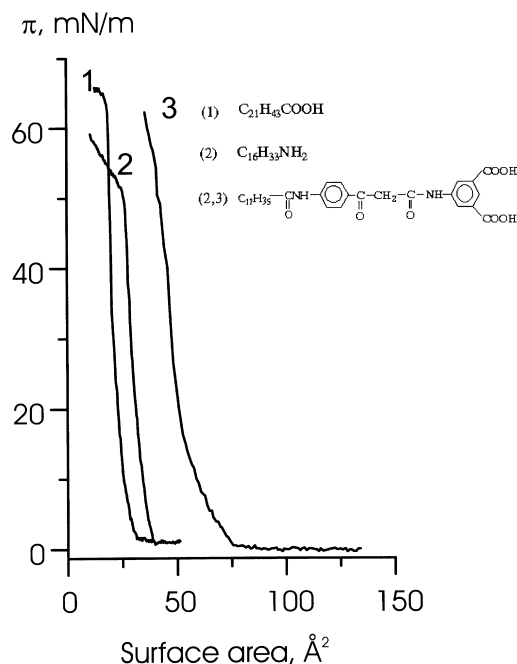


Fig. 1. Compression isotherms (288 K) and corresponding them chemical structures for: (1) behenic acid, (2) mixture of DA : CA = 1 : 2, and (3) DA. All recorded at the CoBr₂ subphase.

1. a cobalt behenate film where closely packed hydrocarbon tails are oriented perpendicular to the substrate;
2. a film of amphiphilic DA molecules lying horizontally on the substrate.

In our experiments, both DA and its mixture with CA revealed excellent surfactant properties on an ionic surface, comparable with those of behenic acid (Fig. 1). The cobalt behenate film was readily obtained by the traditional method (1) using a suitable deposition pressure. The second film was prepared from a mixture of DA and CA using method (2).

Although we paid much attention to the quality of the film prepared on HOPG by method (1), AFM studies revealed that its structure was not perfectly homogeneous. Nevertheless, relatively large areas with a regular structure were imaged. Only a few defects (holes) were observed in the AFM experiment with a Y-type layer of cobalt behenate deposited on HOPG at 30 mN/m. By contrast, the holes covered up to 20% of the surface area in the films deposited at 20 mN/m. A typical Y-type Co-behenate layer is shown in Fig. 2a. The holes were used to determine the layer thickness. A value of about 78 \AA for the 1-Y layer film was obtained. Our measurements indicated a non-stoichiometric extraction of Co²⁺-ions by the molecules of behenic acid (subphase pH 5.8). Since the length of a fully stretched behenic acid molecule is approximately 56 \AA [15], it is possible that Br⁻ ions from subphase may have been partially incorporated into the bilayer. We also found that bilayers and multilayers exhibit better homogeneity and higher ordering than monolayers.

Deposition at 30 mN/m using the modified horizontal lift method (2) produced practically defect-free Z-type mono- and multilayers of cobalt behenate. The monolayers prepared by method (2) at a near collapse pressure revealed remarkable structural reorganization features. Fig. 2b shows the topography of a cobalt behenate film deposited by method (2) at a surface pressure of about 50 mN/m. The stages of double and triple extra-layer formation result in extrusions from the film during compression, which are clearly seen in Fig. 2c.

We have found it very difficult to prepare a high quality monolayer on graphite by the vertical method (1). From our point of view, method (2), which preserves the monolayer structure on an aqueous surface during deposition, gives higher quality monolayers, better suited to scanning probe microscopy.

We did not succeed in obtaining a molecular resolution in AFM imaging of closely packed LB films on HOPG. When

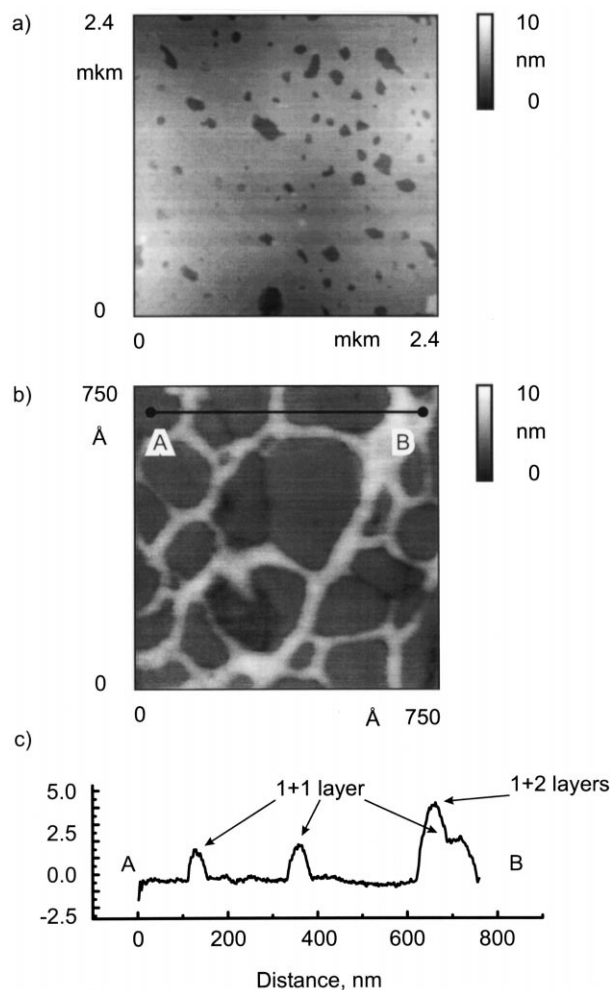


Fig. 2. AFM images of cobalt behenate LB films on HOPG surface taken in the contact mode: (a) 1 Y-type bilayer: deposition method (1) at 20 mN/m; (b) Z-type monolayer and (c) its cross-section: deposition method (2) at 50 mN/m. Hillocks visible on (c) are caused by (1 + 1) bi-layer and (1 + 2) tri-layer formation.

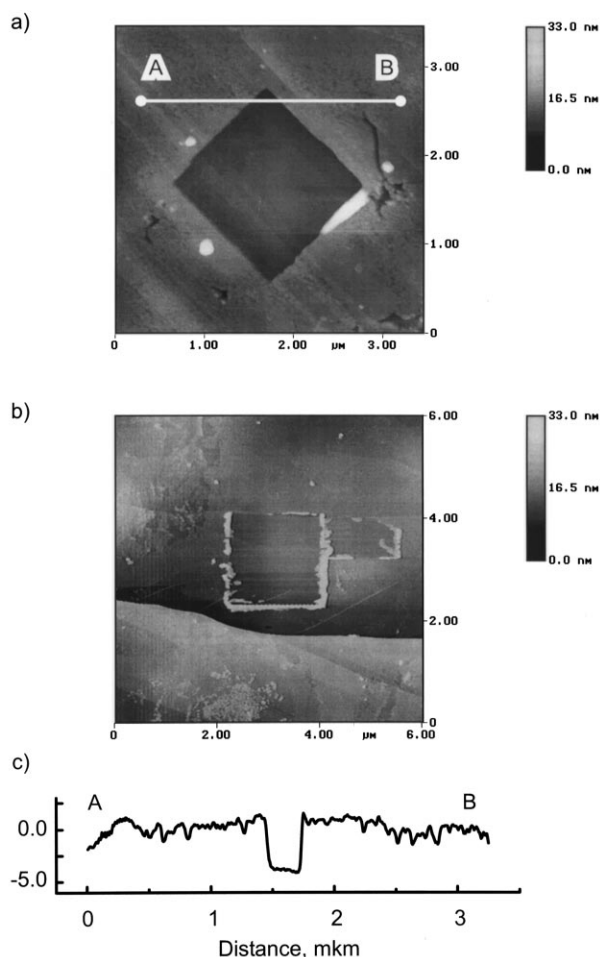


Fig. 3. AFM images of a mixed monolayer DA:CA (1:2, molar ratio): (a) before and (b) after heating in vacuum, (c) cross-section of (a). The monolayer was formed on CoBr_2 subphase at a surface pressure of 30 mN/m and transferred onto the graphite surface. The depth in the scratched area is (a) 28 Å and (b) 3–4 Å.

the image size was reduced to less than $0.5 \times 0.5 \mu\text{m}^2$, the films were easily damaged by the probing tip. This effect may be related to the scan rate reduction, which can be expressed as: $V_{\text{scan}} = L_{\text{image}} \times f_{\text{scan}}$, where L_{image} is the image size and f_{scan} is the scanning frequency (the limitation is imposed by the data digitizing rate $f_{\text{scan}} \leq 60 \text{ Hz}$). For that reason, we used mica surfaces as the substrate in AFM experiments for film molecular lattice visualization.

A bicomponent DA–CA monolayer was deposited on HOPG surface (Fig. 3a) from the ionic subphase using method (2). Using an ionic subphase here is necessary to convert DA molecules into the salt, which we found to be extremely stable at heating. In order to force desorption of CA from the film, we employed the ‘thermal vacuum annealing’ procedure. AFM experiments confirmed (Fig. 3b) that a thin film of organic adsorbate is formed on the substrate after the bicomponent film is heated in vacuum (10^{-4} Torr) at 373 K. The resulting film is characterized

by a horizontal orientation of hydrocarbon tails. Method (1) failed to give a monomolecular covering of the same composition on HOPG.

4.2. STM experiments

The tunneling parameters for STM experiments were carefully adjusted to ensure that the tip did not affect the film surface. The cobalt behenate film surface is shown with a molecular resolution in Fig. 4a. In most cases, images of the bi- and tri-layer cobalt behenate films deposited by method (2) revealed similar features. Experimental STM images suggest a regular two-dimensional arrangement of molecules. Since the STM images were taken with relatively large tunneling gaps, corrugations, usually attributed to metal ions, are not observed here.

We found that the arrangement of cobalt behenate molecules on HOPG surface is best described as a centered rectangular lattice with the following parameters

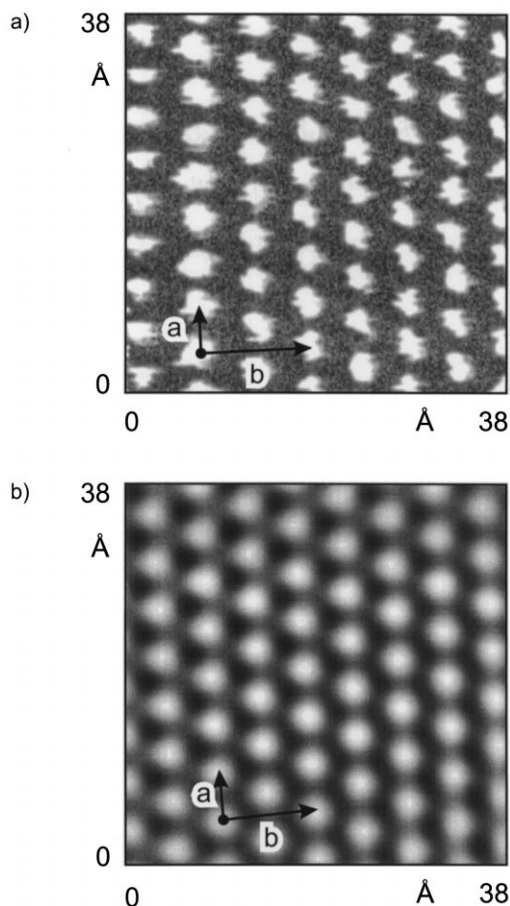


Fig. 4. (a) STM images of cobalt behenate LB film deposited onto graphite (1 bilayer). (b) an AFM image of behenic acid LB film deposited onto mica (1 monolayer). Distances indicated by arrows are: $a = 4.5 \text{ Å}$, $b = 10.5 \text{ Å}$ for (a); $a = 4.7 \text{ Å}$, $b = 8.8 \text{ Å}$ for (b).

$$a = 4.5 \pm 0.4 \text{ \AA}, \quad b = 10.5 \pm 1.0 \text{ \AA},$$

$$b/a = 2.3 \pm 0.3, \quad S = 24 \pm 3 \text{ \AA}^2$$

the deviations are due to calibration errors.

For comparison, molecular AFM image of the behenic acid film (that was obtained even on an monolayer) is shown in Fig. 4b. In order to exclude the thermal drift effect, we determined the lattice parameters by statistical averaging of values obtained from more than 70 AFM images. The lattice can be best described as centered rectangular. The determined parameters for behenic acid film on mica are

$$a = 4.7 \pm 0.2 \text{ \AA}, \quad b = 8.8 \pm 1.0 \text{ \AA},$$

$$b/a = 1.9 \pm 0.2, \quad S = 21.0 \pm 1.8 \text{ \AA}^2$$

the deviations were calculated assuming the Gaussian distribution of data.

We found a good correlation between the experimental ratio of two-dimensional lattice parameters for cobalt behenate: $b/a = 2.3 \pm 0.3$ (STM), behenic acid: $b/a = 1.9 \pm 0.2$ (AFM), and the literature value $b/a \approx 2$ (AFM) for the monolayers of stearates [16]. The packing densities (surface area per molecule) for behenic acids and cobalt behenate were 21.0 ± 1.8 and $24 \pm 3 \text{ \AA}^2$, respectively. This is in a reasonable agree-

ment with the limit surface area of the cobalt behenate film (20.5 \AA^2). We believe that the observed corrugations are aggregates of closely packed vertical alkyl tails.

We calculated tunneling current distributions for the terminal methyl group of a vertically adsorbed octadecane molecule ($\text{C}_{18}\text{H}_{38}$) in its most stable fully stretched conformation. The STM images were simulated under the assumptions that the only molecular orbitals involved in the tunneling process are: (a) the highest occupied molecular orbital (HOMO), (b) the lowest unoccupied molecular orbital (LUMO), (c) all molecular orbitals of the valence electrons. The results for the methyl group are depicted in Fig. 5a–c. Fig. 5c (all valence MO's are involved) and molecular image built on its base (Fig. 5d) are in the best agreement with experiment (Fig. 4a). In order to rationalize this result, we compared the relative energies of the valence MO's to the energy of the Fermi level of graphite. Let the negative ionization potential of octadecane (approximately 9.2 eV) be the zero level. Then the relative energy of the HOMO is -3.0 eV. In fact, the energies of all occupied valence MO's range from -4.5 to -3.0 eV. The relative energy of the LUMO in the EHT description is large positive (9.6 eV). Given that the Fermi levels of graphite is -4.7 eV (the negative value of the work function), it seems reasonable that model (c) is the most appropriate.

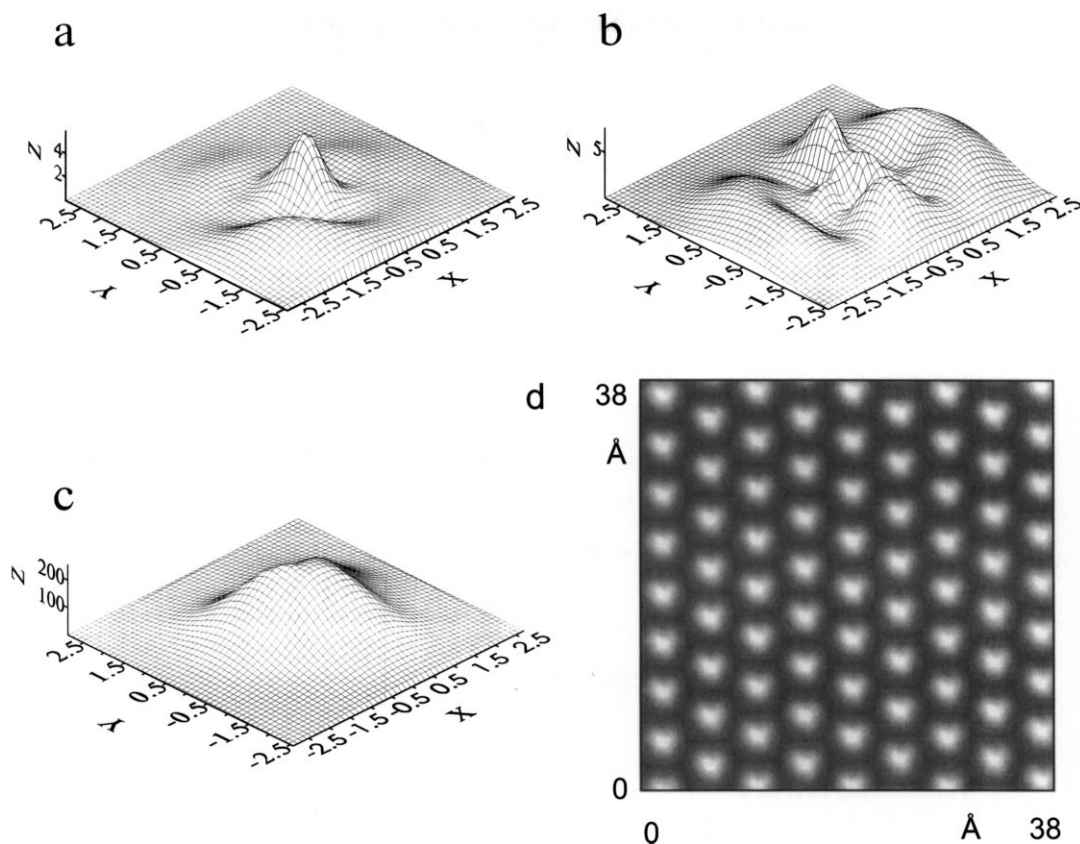


Fig. 5. Contour plots of the constant current through a CH_3 group calculated for (a) HOMO, (b) LUMO, (c) sum of all MO's, (d) reconstruction of the STM image of closely packed methyl groups on a surface.

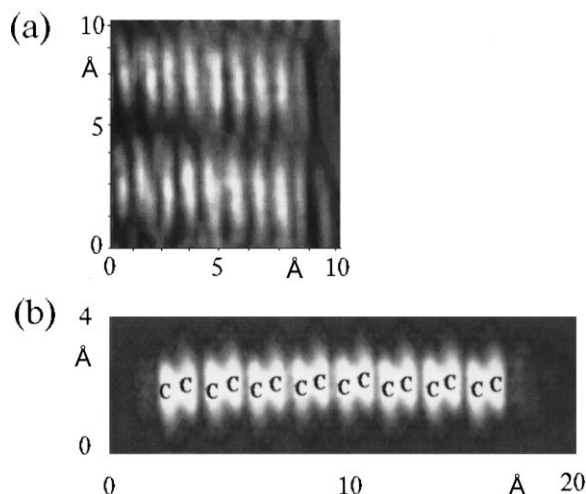


Fig. 6. (a) STM image of two closely lying hydrocarbon tails of DA molecules. The distance between neighboring corrugation maxima is 1.4 Å; (b) calculated contour plot of the constant current (top view: the STM current density for the sum of all molecular orbitals of fiat hydrocarbon tail 1 Å above the molecular plane).

The situation is somewhat different for the horizontal hydrocarbon chains of cobalt behenate prepared by thermal vacuum annealing of a bicomponent mixture (see Fig. 6). In the experimental image, the distance between the neighboring intensity peaks is about 1.4 Å, which indicates that all methylene groups of the alkyl chain are visible. In the simulated image (Fig. 6b) we also observe peaks corresponding to all CH₂ groups, but here the corrugation shapes are different. Apparently, this is due to the mixing of electronic states of organic molecules and the substrate, which is beyond the employed model.

5. Conclusions

A method for preparation of uniform LB film samples for STM imaging has been developed and successfully employed in formation of molecular monolayers. A simple theoretical model of STM images based on calculations of the isolated molecule electron density distribution allows one to make reasonable predictions for STM images of fatty acid compounds on the graphite surface.

References

- [1] L.C. Giancarlo, G.W. Flynn, *Annu. Rev. Phys. Chem.* 49 (1998) 297.
- [2] J.A. DeRose, R.M. Leblanc, *Surf. Sci. Rep.* 22 (1995) 73.
- [3] J. Tersoff, D.R. Hamann, *Phys. Rev. B* 31 (1985) 805.
- [4] P.H. Lippel, R.J. Wilson, M.D. Miller, Ch. Woll, S. Chiang, *Phys. Rev. Lett* 62 (1989) 171.
- [5] H. Ou-Yang, R.A. Marcus, B. Källebring, *J. Chem. Phys.* 100 (1994) 7814.
- [6] H. Ou-Yang, B. Källebring, R.A. Marcus, *J. Chem. Phys.* 98 (1993) 7565.
- [7] H. Ou-Yang, B. Källebring, R.A. Marcus, *J. Chem. Phys.* 98 (1993) 7405.
- [8] V.E. Agabekov, G.K. Zhavnerko, V.N. Staroverov, G. Bar, H.-J. Cantow, *Acta Phys. Pol. A* 93 (1998) 383.
- [9] Yu.N. Moiseev, V.I. Panov, S.V. Savinov, S.I. Vasil'ev, I.V. Yaminsky, *Ultramicroscopy* 42–44 (1992) 1595.
- [10] N. Kunimine, *Soc. Sci. Phot. (Japan)* 14 (1952) 88.
- [11] K.B. Blodgett, I. Langmuir, *Phys. Rev.* 51 (1937) 964.
- [12] R. Hoffmann, *J. Chem. Phys.* 39 (1963) 1397.
- [13] R.S. Mulliken, *J. Chem. Phys.* 45 (1966) 4743.
- [14] R. Rein, N. Fukuda, H. Win, G.A. Clarke, *J. Chem. Phys.* 45 (1966) 4743.
- [15] P. Fromherz, U. Oelschlagel, W. Wilke, *Thin Solid Films* 159 (1989) 421.
- [16] R. Viswanathan, J.A. Zasadzinski, D.K. Schwartz, *Science* 261 (1993) 449.